

A luminescent coordination polymer constructed from fluorene-based bifunctional ligands for the selective detection of tetracyclines and 2,4,6-trinitrophenol

Guiling Wu,^a Chuanzong Dong,^b Pinzhen Liu^a and Chunyang Zheng^{*b}

^a *College of Chemistry and Chemical Engineering, Qiannan Normal University for Nationalities, Duyun 558000, PR China*

^b *Hubei Key Laboratory of Pollutant Analysis and Reuse Technology, College of Chemistry and Chemical Engineering, Hubei Normal University, Huangshi 435002, P. R. China.*

* E-mail: cyzheng@hbnu.edu.cn

CONTENTS

Materials, physical measurement	S3
Fluorescence measurements	S3
Table S1. SHAPE analysis of the Cd ^{II} and Pb ^{II} ions in CP-Cd and CP-Pb	S4
Table S2 Structure of 9 antibiotics.....	S5
Table S3 Structure of 8 phenols.....	S6
Table S4 Comparison of CP-Cd with recent CPs luminescent sensors for TN and CTC.....	S7
Table S5 Comparison of CP-Cd with recent CPs luminescent sensors for TNP.....	S8
Fig. S1 ¹ H NMR of 1 in CDCl ₃	S9
Fig. S2 ¹ H NMR of 2 in CDCl ₃	S9
Fig. S3 ¹³ C NMR of 2 in CDCl ₃	S9
Fig. S4 ¹ H NMR of 3 in CDCl ₃	S10
Fig. S5 ¹ H NMR of 3 in CDCl ₃	S10
Fig. S6 ¹ H NMR of 3 in DMSO-d ₆	S10
Fig. S7 ¹ H NMR spectra of H₂L in DMSO-d ₆	S11
Fig. S8 ¹³ C NMR spectra of H₂L in DMSO-d ₆	S11
Fig. S9 Molecular structure of 3	S12
Fig. S10 Coordination environment of Pb ²⁺ in CP-Pb and 2D network of CP-Pb	S12
Fig. S11 2D Fingerprint plot of H₂L	S12
Fig. S12 2D Fingerprint plot of CP-Cd	S12
Fig. S13 The fluorescence quenching efficiency in 8 different phenols.....	S13
Fig. S14 IR spectra of CP-Cd after sensing different analyte.....	S13
Fig. S15 PXRD patterns of CP-Cd after the detection of analytes.....	S13
Fig. S16 Overlap between the UV of phenols and the EX or EM spectrum of CP-Cd	S14
Fig. S17 The TG curve for CP-Cd under N ₂ atmosphere.....	S14

Materials, physical measurement

all solvents and materials are purchased from Energy Chemical Reagent Co., Ltd. and can be used without any purification. The Single-crystal diffraction data **3**, **H₂L** and **CP-Cd** were collected on a Rigaku Corporation XtaLAB Synergy-I with Cu-K α radiation ($\lambda=1.54184$ Å) and Bruker APEX-II CCD with Mo-K α radiation ($\lambda=0.71073$ Å) for **CP-Pb**. Powder X-ray diffraction (PXRD) measurements were carried out on Bruker D2 Phaser diffractometer with Cu-K α radiation ($\lambda=1.54186$ Å). Thermo gravimetric analysis (TGA) was carried out with a NETZSCH STA 449F5 (TG/DTA) thermal analyzer in temperature region of 25–800 °C with heating rate of 10 °C·min⁻¹ under nitrogen flow. IR spectra of the two compounds were performed on a Bruker AXS TENSOR-27 FT-IR spectrometer (FTIR) with pressed KBr pellets in the range of 4000–400 cm⁻¹. Fluorescence measurements were carried out on an F4700 (Hitachi) fluorescence spectrophotometer at room temperature. UV-vis absorption analysis was performed on a U-3010 spectrophotometer at room temperature. The ¹H and ¹³C NMR spectra were recorded on Bruker AV 300 MHz.

Fluorescence measurements

Well-ground powder of **CP-Cd** (2 mg) was suspended in deionized H₂O (2 mL) using ultrasound for 30 min. For each sensing experiment, a 0.2 mM aqueous solution of antibiotics or phenols solutions were prepared and titrated into the suspension of **CP-Cd** at ambient temperature. Then, the fluorescence emission intensities of different metal ions in the mixed solvent system were measured. The anti-jamming capability of **CP-Cd** was verified by competitive experiments by adding various other analytes (0.2 mM) into **CP-Cd** (2 mg) with a TNP or two tetracyclines (0.2 mM) suspension in 2 mL H₂O after sonication.

Table S1. SHAPE analysis of the Cd^{II} and Pb^{II} ions in **CP-Cd and CP-Pb**

name	label	shape	symmetry	distortion(τ)
CP-Cd	HP-6	Hexagon	D_{6h}	33.327
	PPY-6	Pentagonal pyramid	C_{5v}	13.399
	OC-6	Octahedron	O_h	10.307
	TPR-6	Trigonal prism	D_{3h}	7.791
	JPPY-6	Johnson pentagonal pyramid J2	C_{5v}	17.817
CP-Pb	HP-6	Hexagon	D_{6h}	22.437
	PPY-6	Pentagonal pyramid	C_{5v}	18.514
	OC-6	Octahedron	O_h	18.211
	TPR-6	Trigonal prism	D_{3h}	15.990
	JPPY-6	Johnson pentagonal pyramid J2	C_{5v}	18.612

Table S2 Structure of 9 antibiotics

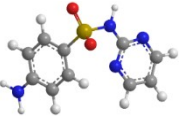
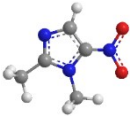
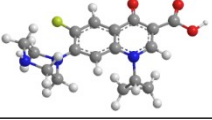
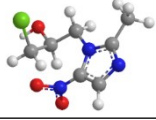
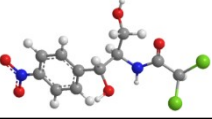
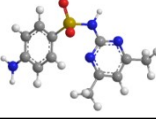
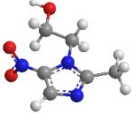
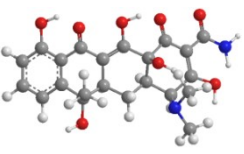
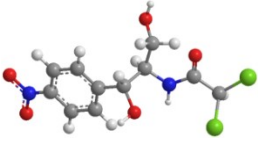
Name	Structure	Name	Structure
Sulfadiazine SDZ		Dimetridazole DTZ	
Ciprofloxacin CPF		Ornidazole ODZ	
Chloramphenicol CAP		Sulfamethazine SMZ	
Metronidazole MDZ		Tetracycline TC	
Chlortetracycline CTC			

Table S2 Structure of 8 phenols

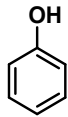
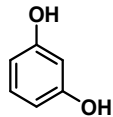
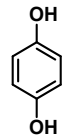
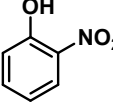
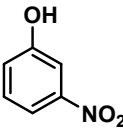
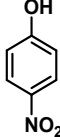
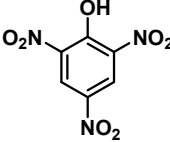
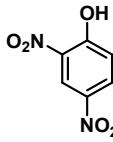
Name	Structure	Name	Structure
phenol PO		m-dihydroxybenzene m-DHB	
p-dihydroxybenzene p-DHB		2-nitrophenol 2-NP	
3-nitrophenol 3-NP		4-nitrophenol 4-NP	
2,4,6-Trinitrophenol TNP		2,4-dinitrophenol DNP	

Table S4 Comparison of CP-Cd with recent LCPs-based luminescent sensors for CTC and TC

LCPs-based chemosensor	Analyst	K_{sv} / M^{-1}	LOD	Medium	Ref.
$\{[Cd(BrBDC)_2(DABCO)_2(DMF)] \cdot 0.5DMF\}_n$	TC	9.87×10^3	2.7 μM	H ₂ O	S1
$[Ni(bim)_2(H_2O)_4](1,5-nds) \cdot (H_2O)_{0.5}$	TC	4.1×10^4	0.82 ppm	H ₂ O	S2
$\{[Zn(2,6-NBC)(H_2O)] \cdot 0.5(H_2O)\}_n$	TC	3.15×10^4	70 nM	H ₂ O	S3
$\{[Cd(HL)(tpytz)(H_2O)]\}_n$	TC	2.776×10^5	0.18 μM	H ₂ O	S4
$\{[Zn(L)_{0.5}(bpy)_{0.5}(H_2O)] \cdot H_2O \cdot DMF\}_n$	TC	6.90×10^4	0.552 μM	H ₂ O	S5
$\{[Tb(\mu_6-Hcaa)(H_2O)]Cl\}_n$	TC	7.12×10^4	0.25 μM	H ₂ O	S6
	CTC	7.51×10^4	0.24 μM	H ₂ O	
CP-Cd	TC	3.24×10^4	0.103 μM	H₂O	this work
	CTC	4.91×10^4	0.098 μM	H₂O	

- S1. A1. S. Datta, P. Ghorai, M. K. Chattopadhyay, N. C. Jana, P. Banerjee, M. H. Mir, *Cryst. Growth Des.*, 2024, **24**, 8645-8654.
- S2. G. Wang, Y.-C. Wang, J. Lu, W.-F. Yan, J. Jin, Y.-P. Wang, J.-J. Zhang, H.-J. Zhang, H. Dong, X.-G. Liu, *Dyes Pigments*, **2024**, *221*, 111832.
- S3. C. Hong, Y.-L. Huang, L. Li, J.-Y. Zou, E.-L. Wang, L. Zhang, Y.-W. Liu, S.-Y. You, *J. Mol. Struct.*, 2024, **1299**, 137113.
- S4. T. Liu, M. Ji, J. Zheng, N. Liu, H. Hao, J. Dou, J. Jiang, Y. Li, S. Wang, *J. Mater. Chem. C* 2024, **12**, 17635-17646.
- S5. L. Wang, T. Liu, J. Cheng, H. Zou, J. Lu, H. Liu, Y. Li, J. Dou, S. Wang, *J. Mol. Struct.*, 2024 **1296**, 136815.
- S6. Y. Zhang, A. Wang, S. Feng, C. Yuan and L. Lu, *Dalton Trans.*, 2023, **52**, 5243-5251.

Table S5 Comparison of **CP-Cd** with recent LCPs-based luminescent sensors for TNP

LCPs-based chemosensor	K_{sv} / M^{-1}	LOD	Medium	Ref.
CdMOF-NH ₂	2.1×10^4	0.031 μ M	H ₂ O	S7
ZnMOF-NH ₂	2.23×10^4	0.045 μ M		
{[Eu ₆ L ₆ (μ -OH) ₈ (H ₂ O) ₃] ₈ ·H ₂ O} _n }	1.92×10^4	1.93 μ M	DMF	S8
[Zn ₂ (tdc) ₄ (pdic) ₃]	0.8×10^5	0.154 μ M	H ₂ O	S9
[Cd ₃ (H ₂ O)(H ₃ L) ₂ (dia) ₂]·4DMA·10H ₂ O	1.43×10^5	NR	H ₂ O	S10
[Zn-(PBBA)(H ₂ O)]·3DMF·2H ₂ O	4.4×10^4	1.0 μ M	H ₂ O	S11
CP-Cd	4.77×10^4	0.147 μM	H₂O	This work

- S7. M. Kaur, M. Yusuf, Y. F. Tsang, K. H. Kim, A. K. Malik, *Sci Total Environ.*, 2023, **857**, 159385.
- S8. Y. Zhao, C. A. Wang, J. K. Li, Q. L. Li, Q. Guo, J. Ru, C. L. Ma, Y. F. Han, *RSC Adv.*, 2022, **12**, 26945-26952.
- S9. G. Bairy, A. Dey, B. Dutta, S. Maity, C. Sinha, *Dalton Trans.*, 2022, **51**, 13749-13761
- S10. Q. An, S. Bao, X. Li, J. Sun and Z. Su, *New J. Chem.*, 2022, **46**, 11377-11381.
- S11. W. Liu, J. Qiao, J. Gu and Y. Liu, *Inorg. Chem.*, 2023, **62**, 1272-1278.

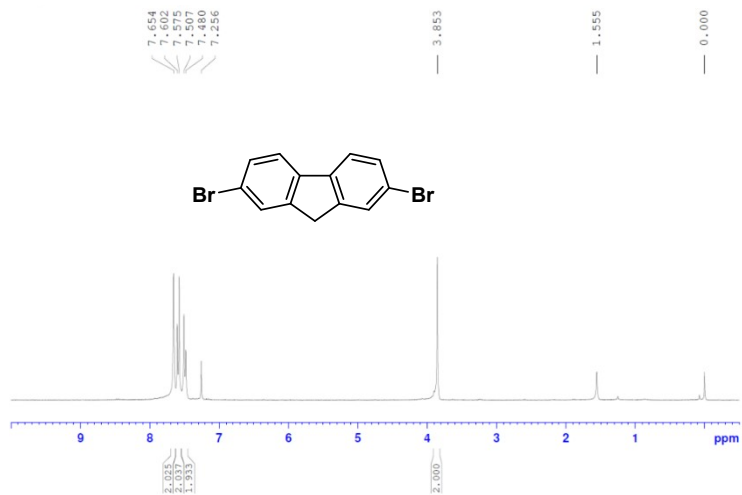


Fig.S1 ¹H NMR spectra of **1** in CDCl₃

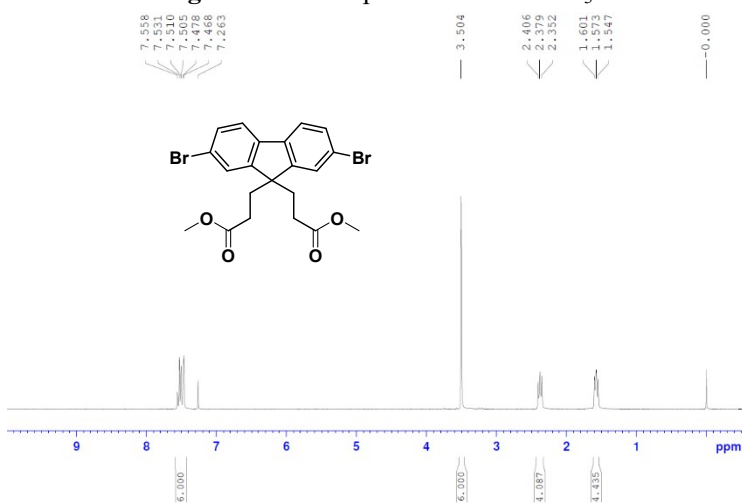


Fig. S2 ¹H NMR spectra of **2** in CDCl₃



Fig. S3 ¹³C NMR spectra of **2** in CDCl₃

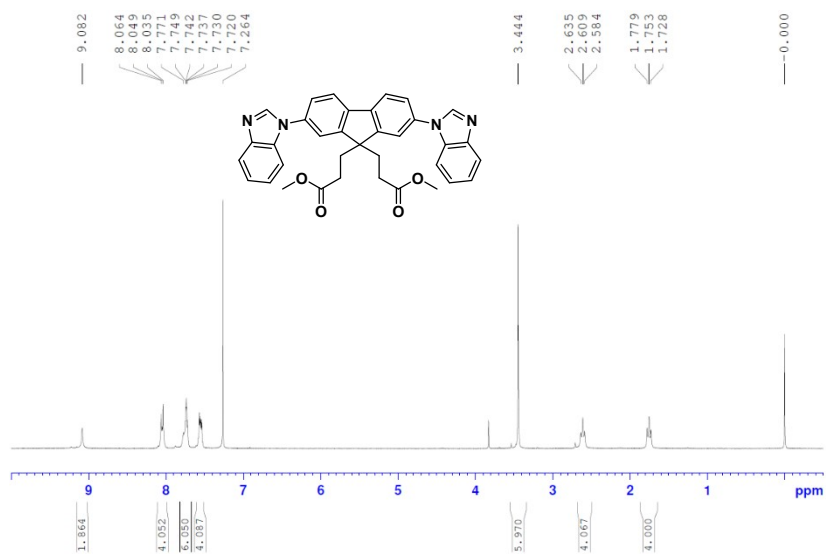


Fig. S4 ¹H NMR spectra of **3** in CDCl₃

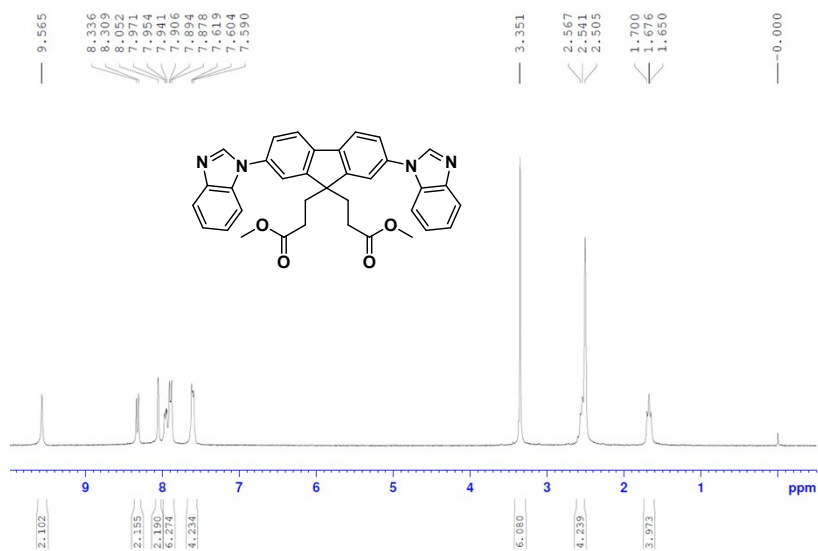


Fig. S5 ¹H NMR spectra of **3** in DMSO-d₆

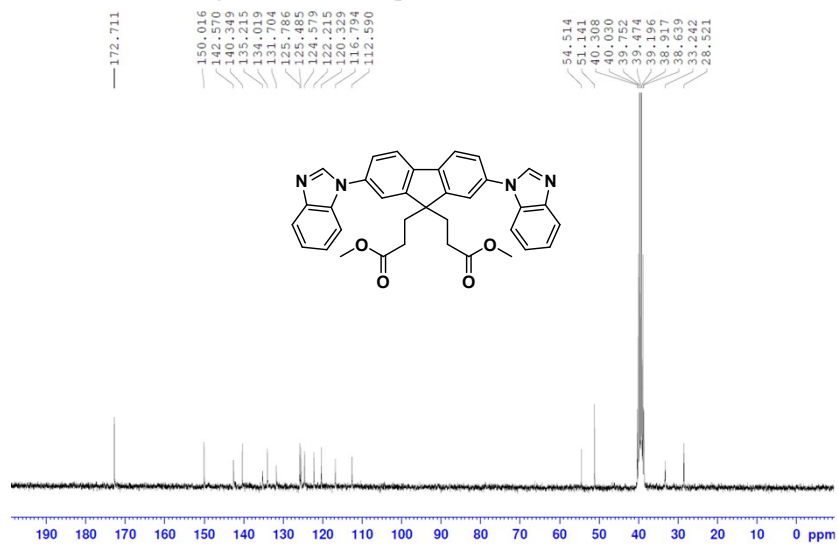


Fig. S6 ¹³C NMR spectra of **3** in DMSO-d₆

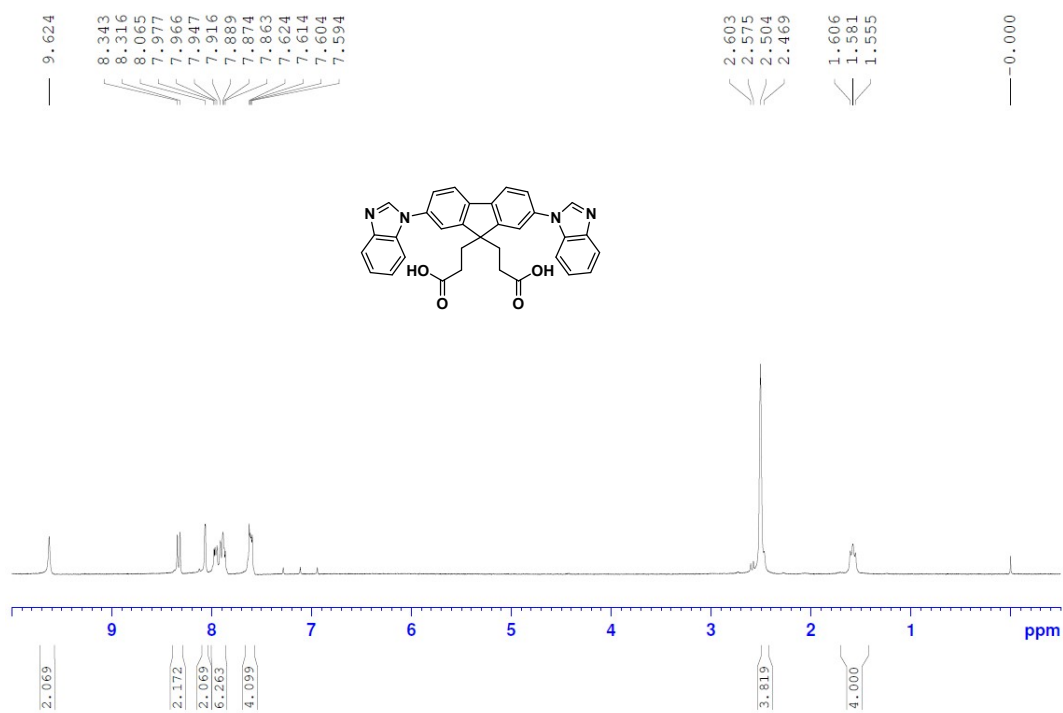


Fig. S7 1H NMR spectra of H_2L in $DMSO-d_6$

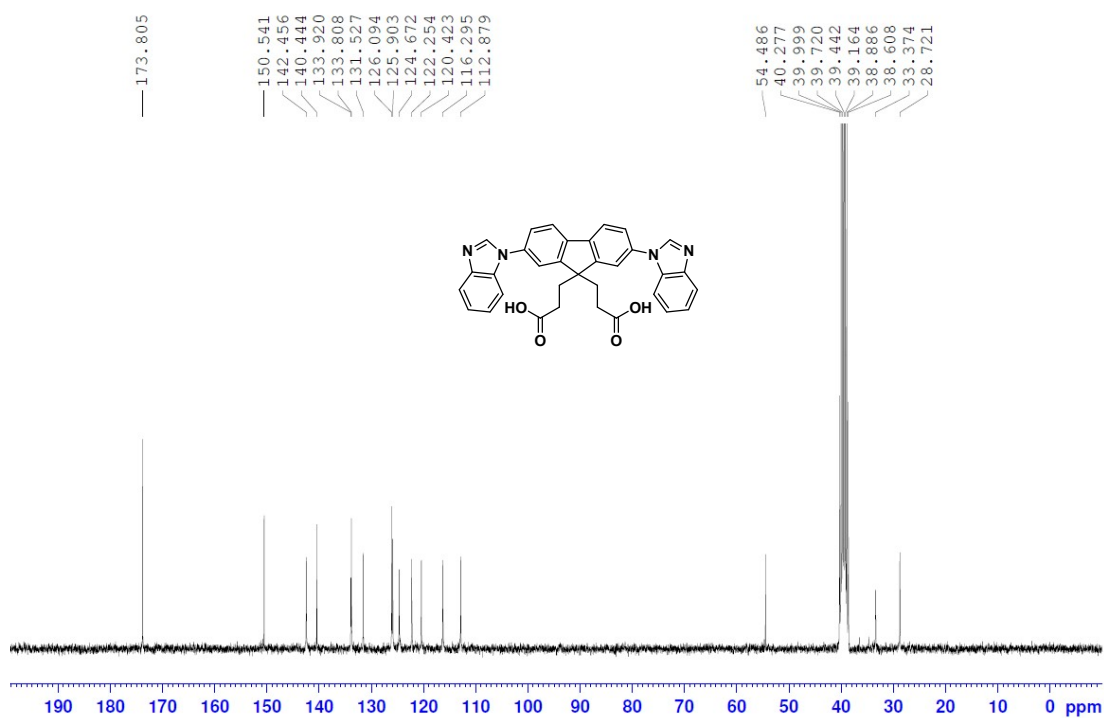


Fig. S8 ^{13}C NMR spectra of H_2L in $DMSO-d_6$

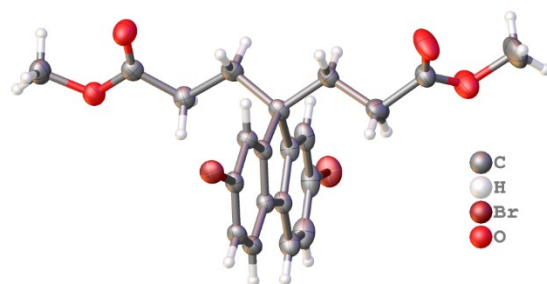


Fig. S9 Molecular structure of 3

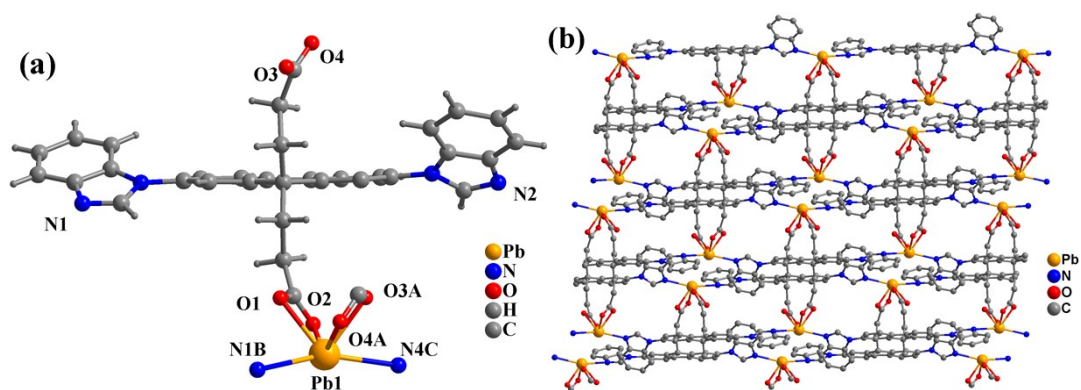


Fig. S10 (a) Coordination environment of Pb^{2+} in CP-Pb;
(b) 2D network assembly diagram of CP-Pb

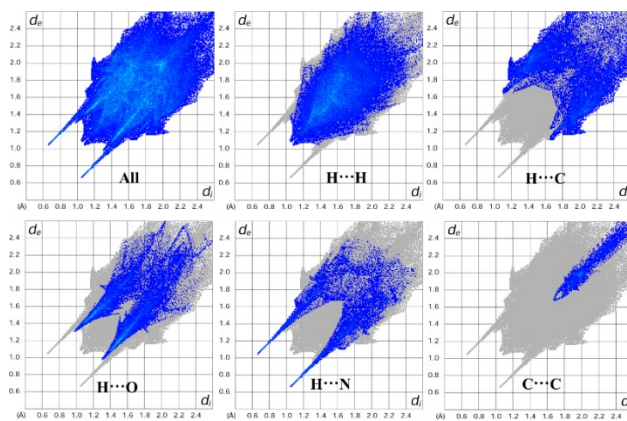


Fig. S11 2D Fingerprint plot of H_2L

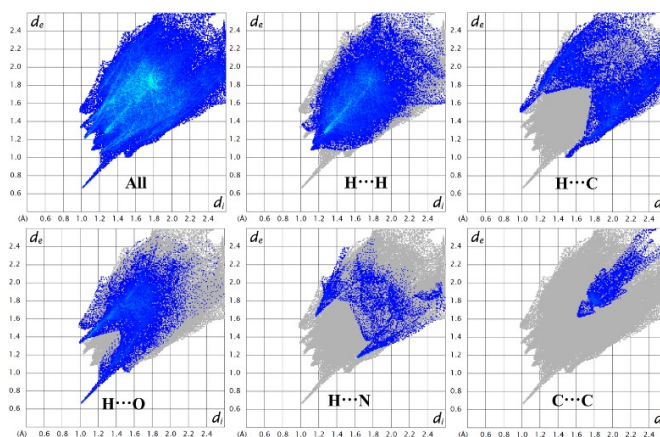


Fig. S12 2D Fingerprint plot of CP-Cd

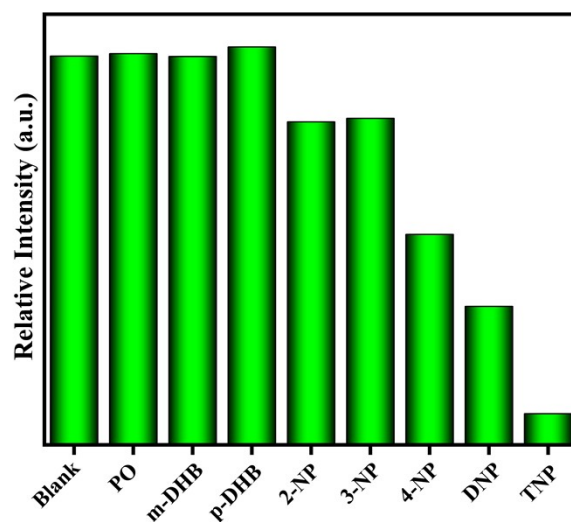


Fig. S13 The percentage of fluorescence quenching efficiency in 8 different phenols

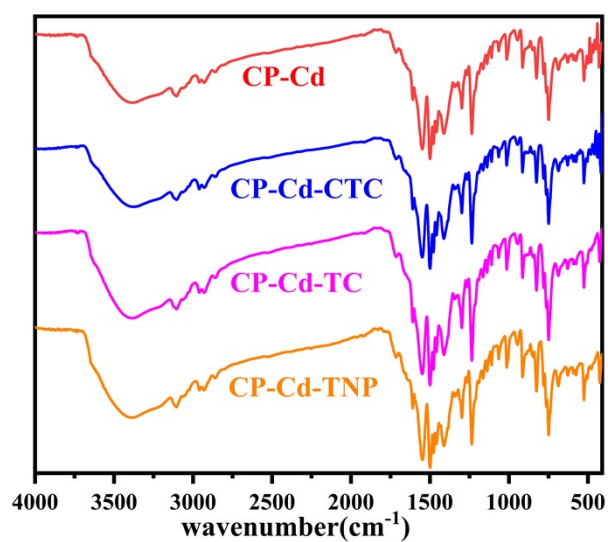


Fig. S14 IR spectra of CP-Cd after sensing different analytes

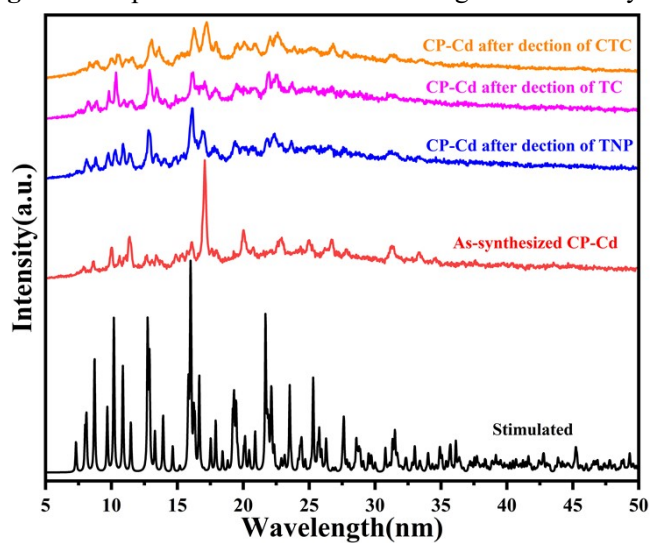


Fig. S15 PXRD patterns of CP-Cd after the detection of analytes

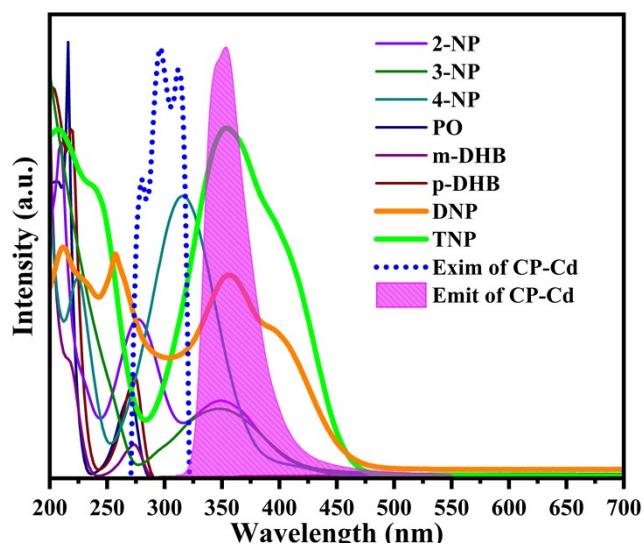


Fig. S16 Overlap between the UV absorption spectra of various phenols and the excitation or emission spectrum of CP-Cd

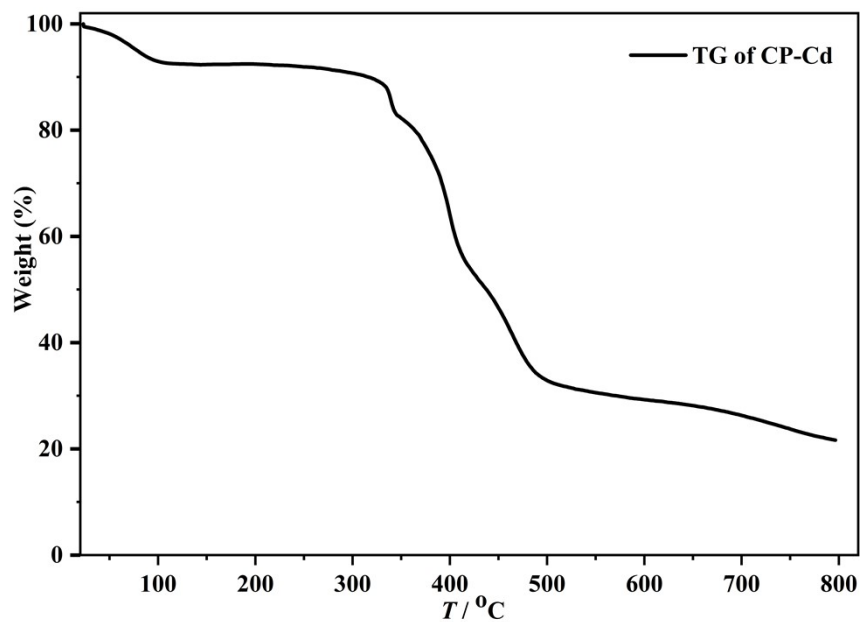


Fig. S17 The TG curve for CP-Cd under N₂ atmosphere